Fibroblast growth factor-2 drives and maintains progressive corneal neovascularization following HSV-1 infection

HR Gurung[1], MM Carr[2], K Bryant[2], AJ Chucair-Elliott[2] and DJJ Carr[1,2]

Herpes simplex virus type 1 (HSV-1) infection of the cornea induces vascular endothelial growth factor A (VEGF-A)-dependent lymphangiogenesis that continues to develop well beyond the resolution of infection. Inflammatory leukocytes infiltrate the cornea and have been implicated to be essential for corneal neovascularization, an important clinically relevant manifestation of stromal keratitis. Here we report that cornea infiltrating leukocytes including neutrophils and T cells do not have a significant role in corneal neovascularization past virus clearance. Antibody-mediated depletion of these cells did not impact lymphatic or blood vessel genesis. Multiple pro-angiogenic factors including IL-6, angiopoietin-2, hepatocyte growth factor, fibroblast growth factor-2 (FGF-2), VEGF-A, and matrix metalloproteinase-9 were expressed within the cornea following virus clearance. A single bolus of dexamethasone at day 10 post infection (pi) resulted in suppression of blood vessel genesis and regression of lymphatic vessels at day 21 pi compared to control-treated mice. Whereas IL-6 neutralization had a modest impact on hemangiogenesis (days 14–21 pi) and lymphangiogenesis (day 21 pi) in a time-dependent fashion, neutralization of FGF-2 had a more pronounced effect on the suppression of neovascularization (blood and lymphatic vessels) in a time-dependent, leukocyte-independent manner. Furthermore, FGF-2 neutralization suppressed the expression of all pro-angiogenic factors measured and preserved visual acuity.

INTRODUCTION

The cornea is an immune privileged tissue and its transparency is critical for optimal visual acuity. The avascular nature of the cornea otherwise known as angiogenic privilege further corroborates its immune privilege status.[1] It is a well-accepted concept that a fine balance between the activity of angiogenic and anti-angiogenic factors in the cornea are critical in maintaining its avascularity.[1–3] Several studies indicate that the presence of the blood–ocular barrier, low major histocompatibility complex-class I-expressing cells, immature antigen presenting cells (APCs), CD95 ligand expression on endothelial and epithelial cells, immunosuppressive microenvironment of the anterior chamber, and lack of lymphatic vessels in the cornea, all play a co-operative role in minimizing immune responses to antigens that the cornea encounters on a daily basis.[1,4,5]

Angiogenic privilege of the cornea can be lost as a result of trauma, injury, or infection. While the first-line treatment for corneal neovascularization is topical administration of steroid or non-steroid anti-inflammatory drugs, unwarranted side effects can occur especially following long-term application.[3] Corneal transplantation is often undertaken to maintain continuity of visual acuity. Despite the 5 years graft success rate of 70% for corneal transplant, infection-related complications account for about 30% of the failed transplant cases. Herpes simplex virus type 1 (HSV-1) infection of the cornea is one of the main causes of such transplant-related complications.[6] As such, HSV-1 is the leading cause of infectious corneal blindness in the developed world with seroconversion of at least 60% of the world population.[7]

HSV-1 infection of the mouse cornea has been shown to induce hemangiogenesis and lymphangiogenesis.[8] Inflammatory lymphangiogenesis requires vascular endothelial growth factor (VEGF)-C production and involvement of CD11b-positive macrophages.[9,10] However, HSV-1-induced corneal

[1]Department of Microbiology and Immunology, University of Oklahoma Health Sciences Center, Oklahoma City, Oklahoma, USA and [2]Department of Ophthalmology, University of Oklahoma Health Sciences Center, Oklahoma City, Oklahoma, USA. Correspondence: DJJ Carr (dan-carr@ouhsc.edu)

Received 30 August 2016; accepted 24 February 2017; published online 5 April 2017. doi:10.1038/mi.2017.26

lymphangiogenesis does not require VEGF-C, VEGF receptor 3 (VEGFR3), or infiltrating macrophages.[8] Rather, it is dependent on VEGF-A production by infected epithelial cells that act via VEGFR2.[8] VEGF-A is driven by the HSV-1 immediate-early gene product, infected cell protein 4, that binds to guanine cytosine-enriched sites within the VEGF-A promoter.[11] One exception has been noted in a transgenic $CD8^+$ T-cell receptor (gBT-I.1) model of HSV-1-induced ocular lymphangiogenesis. In that model, it was noted the $CD8^+$ T cells were a significant source of VEGF-A and VEGF-C and furthermore, VEGF-C neutralization severely reduced lymphatic growth in the corneas of HSV-1-infected gBT-I.1 transgenic mice.[12] Although the gBT-I.1 mouse model is unusual, it nevertheless underscores the likelihood of additional sources of pro-angiogenic factors driving lymphatic vessel growth under unique pathological conditions.

Although the observations described above occur during acute infection, a conundrum exists in which neovascularization including lymphangiogenesis continues to develop well past the clearance of the virus.[8] Another lab has described the contribution of pro-inflammatory cytokines, matrix metalloproteinase-9 (MMP-9), and infiltrating neutrophils in HSV-1-induced corneal neovascularization.[13–15] However, the relative contribution of infiltrating leukocytes including neutrophils in corneal lymphangiogenesis following virus resolution has not been described.

Here we report neutrophils are dispensable for the development and maintenance of blood and lymphatic vessels in the cornea following the clearance of HSV-1. Specifically, a single bolus of dexamethasone (DEX) at the time of virus clearance had a profound impact on the suppression of neovascularization that was associated with an impressive reduction in the expression of multiple pro-angiogenic factors but not neutrophil infiltration. Among the pro-angiogenic factors impacted by DEX at times post infection (pi), we identified fibroblast growth factor-2 (FGF-2) as the leading candidate. Neutralization of FGF-2 blocked corneal neovascularization associated with a loss of pro-angiogenic factors but not MMP-9 or neutrophil infiltration. Anti-FGF-2 antibody treatment was also found to partially preserve visual acuity in HSV-1-infected mice but had no effect on corneal sensitivity. Collectively, the results suggest FGF-2 is a critical factor in the long-term

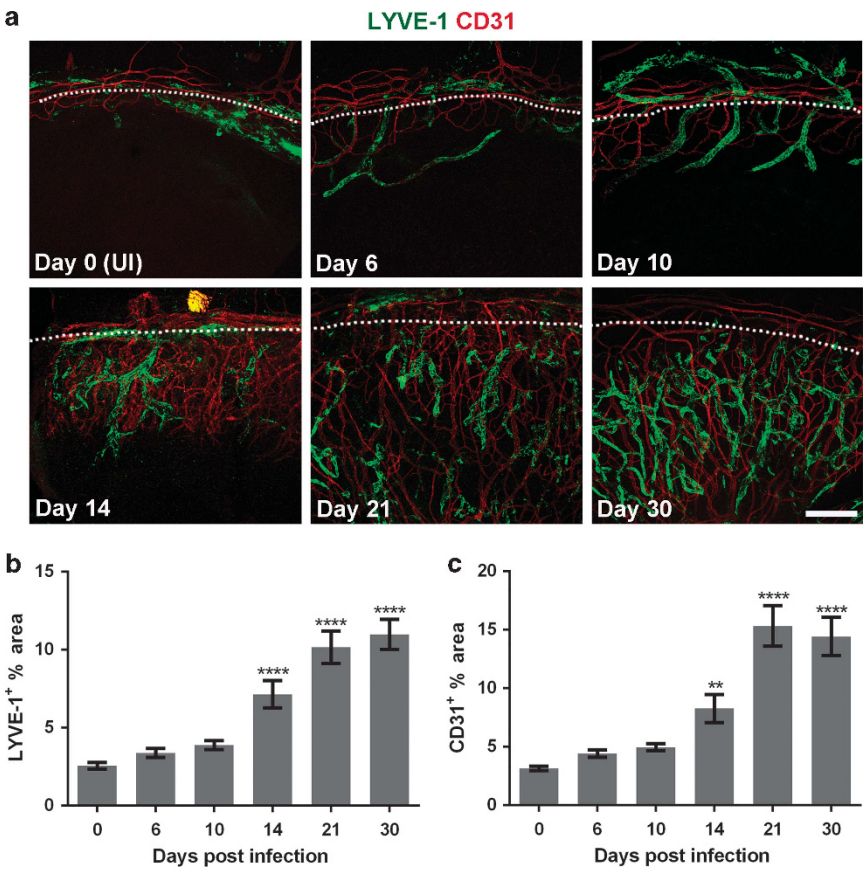

Figure 1 Progressive development and maintenance of HSV-1-induced corneal neovascularization post-virus clearance. Mice were inoculated with HSV-1 onto the killed corneas, and at indicated days post infection (pi) the corneas were collected, stained, and mounted *en face* on slides for image capture and analysis. (**a**) Representative images of the corneas with lymphatic (green) and blood (red) vessels at indicated days pi. Each image represents a Z-stacked quadrant of a cornea. White dotted lines demarcate the limbal region from the cornea proper. Bar = 200 μm. (**b**) Metamorph quantification of the corneal area containing lymphatic vessels. (**c**) Metamorph quantification of the corneal area containing blood vessels. Data represent summary of mean ± s.e.m. of two independent experiments with $n = 10–12$ corneas per time point. $^{**}P<0.01$, $^{***}P<0.001$, $^{****}P<0.0001$ comparing infected mice to UI control animals as determined by one-way ANOVA followed by Dunnett's multiple comparisons test. UI, uninfected.

maintenance of newly acquired corneal blood and lymphatic vessels in response to HSV-1 infection. Targeting FGF-2 may be an additional adjunct therapy to currently prescribed intervention to preserve the visual axis as it relates to HSV-1 infection.

RESULTS

Dynamics of HSV-1-induced corneal lymphangiogenesis that persists well beyond virus resolution

HSV-1 infection of murine cornea induces VEGF-A-dependent lymphangiogenesis that persists well beyond the clearance of the virus from the cornea.[8] In order to determine the dynamics of corneal lymphangiogenesis following virus clearance from the cornea, a time-course analysis of lymph- and hem-angiogenesis was undertaken. We found a pattern of continuous development up to day 21 pi and then maintenance of lymph- and hem-angiogenesis in the cornea up to day 30 pi (**Figure 1a–c**). Blood and lymphatic vessels continue to grow and persist after the clearance of virus from the cornea up to at least day 120 pi (unpublished observation).

Neutrophils do not contribute to HSV-1-induced corneal neovascularization

Following HSV-1 infection of the cornea, inflammatory cells including neutrophils, monocytes, macrophages, and T cells infiltrate the central cornea.[16–18] These cells are a tremendous source of growth factors and cytokines that can induce angiogenesis. In particular, there is precedence in the literature that suggests the role for infiltrating neutrophils in HSV-1-induced corneal hemangiogenesis.[13] In order to test the hypothesis that infiltrating neutrophils also induce lymphangiogenesis following HSV-1 infection, we performed a time-course experiment to determine the dynamics of infiltrating leukocytes along with antibody-mediated depletion of neutrophils on corneal lymphangiogenesis. Flow cytometric analysis of corneas revealed a progressive infiltration of leukocytes including neutrophils, inflammatory monocytes, macrophages, $CD4^+$ T cells, $CD8^+$ T cells, and natural killer (NK) cells (**Figure 2a**). The peak infiltration of all leukocyte populations with the exception of macrophages occurred at day 14 pi, and remained elevated at day 30 pi (**Figure 2a**). By comparison, the infiltration of macrophages peaked at day 10 pi (**Figure 2a**). Further analysis of infiltrating cell localization within the cornea using 3-dimensional (3D) deconvolution of Z-stacked corneas showed predominant extravascular/posterior stroma localization (**Figure 2b** and **Supplementary Video1.mov online**). We next evaluated the contribution of neutrophils to the development of lymphatic vessels using anti-Ly6G monoclonal antibody to target neutrophils. Although anti-Ly6G antibody-treated mice exhibited a selective depletion of neutrophils in the circulation, it did not induce any appreciable depletion of infiltrating neutrophils in the cornea and was dropped from further consideration (data not shown). Consequently, we employed anti-Gr1 monoclonal antibody that has a broader coverage to deplete infiltrating neutrophils post HSV-1 infection. Anti-Gr1 antibody-treated mice not only exhibited a profound depletion of circulating neutrophils but also a significant loss of peripheral NK cells and $CD3^+$ T cells (**Figure 3a,b**). The antibody also induced a remarkable depletion of infiltrating neutrophils and T cells but not NK cells or monocytes/macrophages in the cornea at day 14 pi (**Figure 3c,d**). However, the depletion of infiltrating neutrophils did not appear to have any appreciable effect on corneal lymph- and hem-angiogenesis at this time point (**Figure 3e–g**). We interpret these results to suggest infiltrating leukocytes including neutrophils and T cells following HSV-1 clearance do not have a significant role in the progressive development and maintenance of corneal neovascularization.

Expression of pro-angiogenic factors in the cornea after virus clearance

Next, we performed time-course experiments to probe for gene expression of several pro-angiogenic factors including IL1-β, IL-6, MMP-9, VEGF-A, PROX-1, VEGF-C, MMP-2, ANGPT-2, IL-17F, LT-α, CCL21-α, TNF-α, PDGF-β, hepatocyte growth factor (HGF), FGF-2, NOTCH1, IGF-2, LT-β, and ANGPT-1.[19–21] IL1-β gene expression was significantly elevated at day 14 pi (**Figure 4a,d**) as was VEGF-A, PROX-1 (**Figure 4b,d**), LT-β, and TNF-α (**Figure 4c,d**). The latter group expression peaked at day 10 pi. Among the pro-angiogenic factors assayed for expression at the protein level, IL-6, Ang-2, FGF-2, HGF, VEGF-A, and MMP-9 were all elevated at times pi (**Figure 4e–j**). Specifically, the expression of these factors peaked at day 14 pi with the exception of FGF-2 that peaked at day 21 pi (**Figure 4g**). MMP-9 expression peaked at day 10 pi and remained elevated through day 21 pi (**Figure 4j**). However, the expression of all of the pro-angiogenic factors tapered off by day 30 pi to levels similar to those found in uninfected controls (**Figure 4e–j**). VEGF-C, TNF-α, and IL-1β protein levels were also evaluated but the expression was inconsistently detected and statistically not above uninfected controls (data not shown). We interpret these results to suggest that the expression of some or all of these pro-angiogenic factors promotes the continued genesis and maintenance of blood and lymphatic vessels in the cornea following virus clearance.

DEX suppresses HSV-1-induced corneal neovascularization in a time-dependent manner

Previous results have reported the anti-angiogenic effects of DEX on corneal neovascularization in response to trauma.[22,23] Therefore, DEX was investigated for global anti-inflammatory effects including neovascularization in the cornea in response to HSV-1 infection. To circumvent the potent immunosuppressive effects of DEX during acute HSV-1 infection that would likely result in the death of treated mice and begin to address the factors/cells that contribute to corneal angiogenesis following viral clearance, DEX treatment was initiated at the time of virus resolution from the cornea. A single bolus of DEX administered at day 10 pi was found to significantly suppress further development of blood but not lymphatic vessels day 14 pi (**Figure 5a–c**). Multiplex suspension array on the corneas at day 14 pi revealed a significant drop in IL-6, Ang-2, HGF, and VEGF-A, but not FGF-2 and MMP-9 protein levels

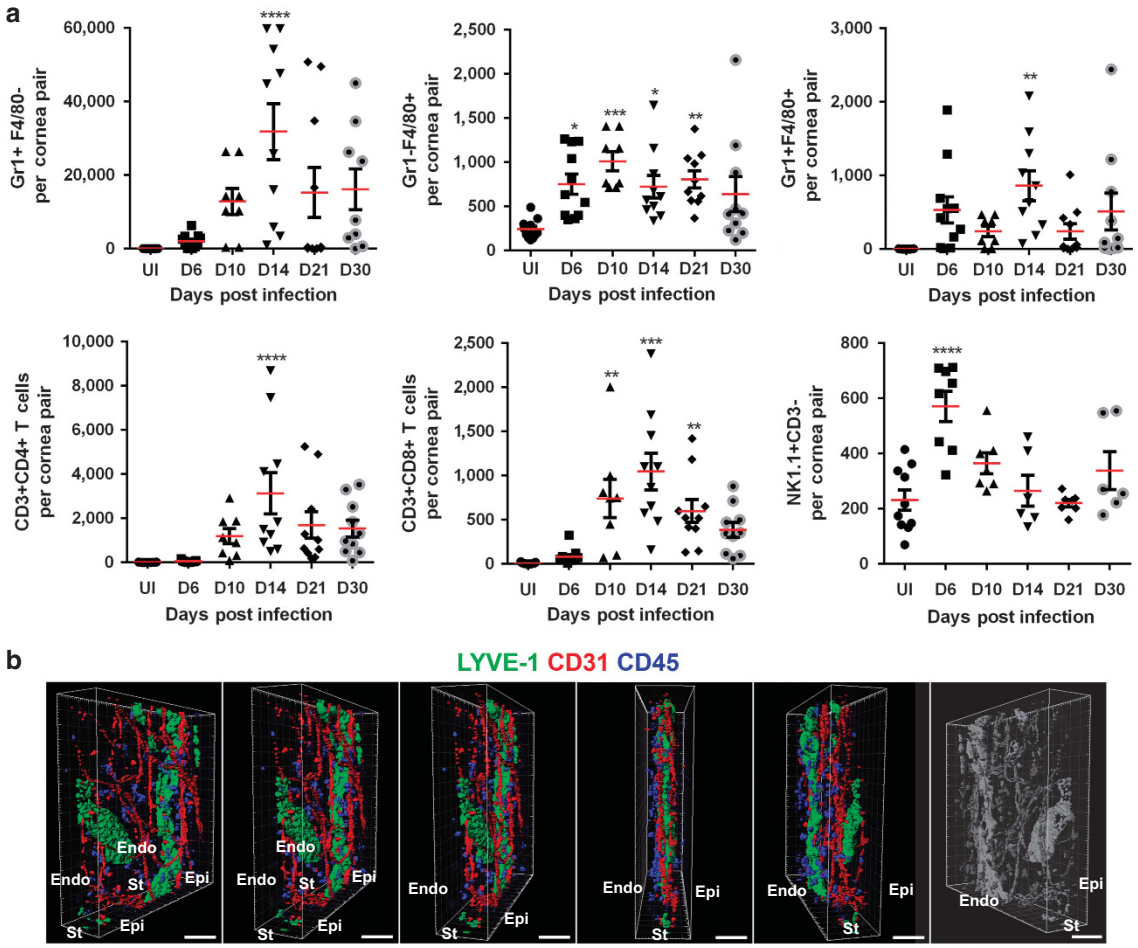

Figure 2 Leukocytes infiltrate the cornea beyond the resolution of HSV-1 infection. Mice were inoculated with HSV-1 and the corneas were excised at the indicated times post infection. (**a**) Flow cytometric analysis results of Gr1 + F4/80 − (neutrophils), Gr1 + F4/80 + (inflammatory monocytes), Gr1-F4/80 + (macrophages), $CD3^+CD4^+$ T cells, $CD3^+CD8^+$ T cells, and $NK1.1^+CD3^-$ (natural killer, NK) cells are included. (**b**) Representative Z-stacked 3D still images of a highly vascularized cornea from a day 30 post infected mouse indicating lymphatic vessels (green), blood vessels (red), and CD45 + leukocytes (blue). Each image is a snapshot of a 3D cornea as it rotates clockwise showing endothelium (Endo), stroma (St), and epithelium (Epi). Bars = 50 μm. Results indicate summary of mean ± s.e.m. of two independent experiments with $n = 8$–10 mice per time point. $^*P<0.1$, $^{**}P<0.01$, $^{***}P<0.001$, $^{****}P<0.0001$ comparing infected mice to uninfected (UI) control animals as determined by one-way ANOVA and Dunnett's multiple comparisons test.

(**Figure 5d**). When the experiment was extended to day 21 pi following a single bolus of DEX at day 10 pi, there was a remarkable regression of blood and lymphatic vessels down to levels observed in uninfected controls (**Figure 5e–g**). Strikingly, the analysis of pro-angiogenic factor expression in the cornea at day 21 pi revealed a profound suppression of HGF and VEGFA as well as MMP-9 and FGF-2 in response to DEX treatment (**Figure 5h**). Notably, although DEX induced a significant downregulation of MMP-9 expression, the expression of this enzyme was still significantly above the level in uninfected corneas (**Figure 5h**). Furthermore, it was of interest to note DEX treatment did not alter the total number of infiltrating leukocytes residing in the cornea despite a loss in vessel genesis (**Figure 5i**).

Since a previous study suggested a role for MMP-9 in HSV-1-induced corneal hemangiogenesis[14] and DEX-induced suppression of neovascularization (**Figure 5a,e**) correlated with a significant loss in MMP-9 expression (**Figure 5h**), we investigated the contribution of MMP-9 in HSV-1-induced lymphangiogenesis. The results show MMP-9-deficient corneas exhibited no appreciable difference in lymph- or hem-angiogenesis compared to infected wild-type mice when assessed at day 14 pi (**Figure 6a–c**). We interpret the results to suggest MMP-9 alone does not contribute to HSV-1-induced corneal neovascularization during acute or latent infection but rather, other pro-angiogenic cytokines may, contribute to the progression and maintenance of the corneal vessels in response to virus.

IL-6 neutralization blocks progression of HSV-1-induced blood and lymphatic vessels in the infected cornea

IL-6 has previously been reported to induce VEGF through a synergistic effect between 5′-untranslated region elements located upstream of the transcription initiation site.[24] As IL-6 is

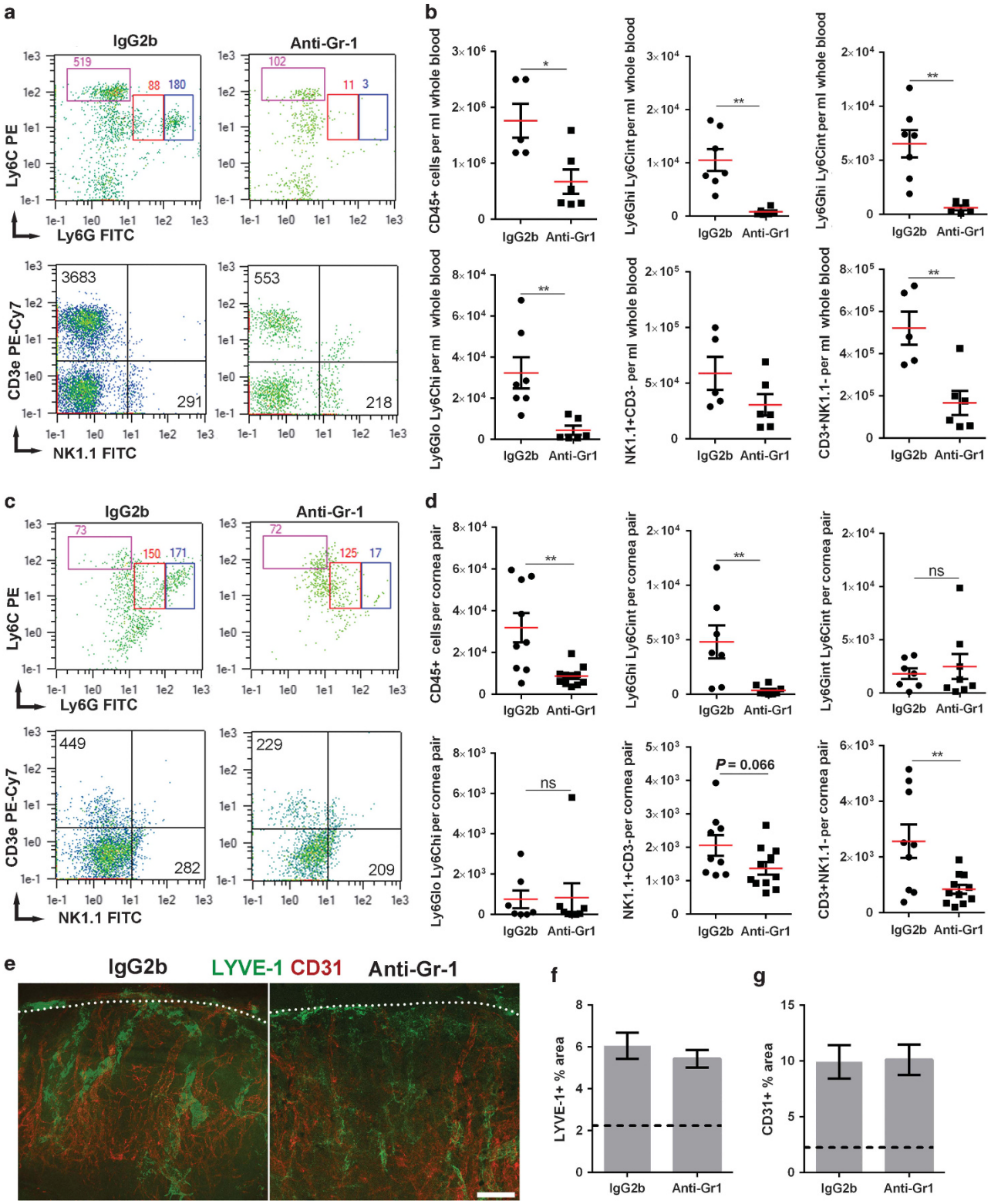

Figure 3 Anti-Gr1 antibody depletes neutrophils in the cornea but does not have an appreciable impact on corneal neovascularization. (**a**) Representative flow cytometry plots indicating myeloid cells, CD3 + NK1.1 − T cells, and NK cells in the blood at day 14 post infection (pi) comparing isotype control antibody-treated mice to Gr1-depleting antibody-treated animals. Myeloid cells were gated on CD45 + CD3 − CD11b + population. (**b**) Quantification of leukocytes in the blood at day 14 pi following antibody administration. (**c**) Representative flow cytometric plots indicating myeloid cells, NK cells, and T cells at day 14 pi comparing isotype control antibody-treated mice to anti-Gr1 antibody-treated mice. (**d**) Quantification of infiltrating leukocytes in the cornea at day 14 pi post antibody treatment. (**e**) Representative images of Z-stacked corneas at day 14 pi comparing isotype control antibody-treated mice to anti-Gr1 antibody-treated animals. (**f**,**g**) Metamorph quantification of corneal area containing lymphatic (green) and blood (red) vessels per × 100 field of view. Bar = 200 μm. Data represent summary of mean ± s.e.m. of two independent experiments with $n = 5–8$ mice (**a**,**b**), $n = 5–6$ mice (**c**–**g**). $^{*}P < 0.05$, $^{**}P < 0.01$, $^{***}P < 0.001$, as determined by Student's *t*-test.

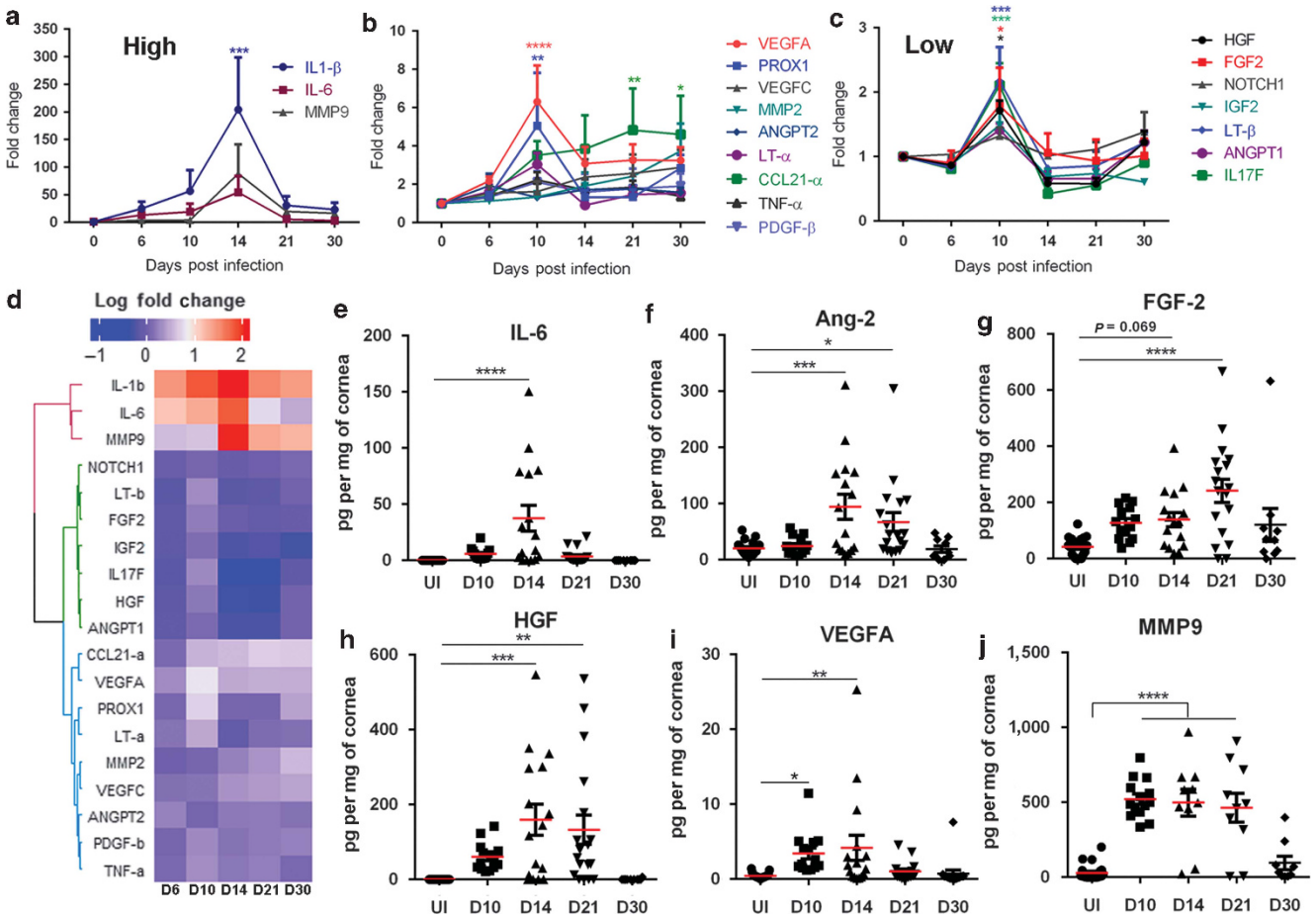

Figure 4 Gene and protein expression of pro-angiogenic factors are elevated in the cornea following virus clearance. Mice were infected with HSV-1 and corneas were collected at the indicated times post infection (pi) to for gene and protein expression analysis. Gene expression is categorized as (**a**) high relative expression, (**b**) medium relative expression, and (**c**) low relative expression in the corneas at times pi. (**d**) Heat map clustering/analysis of pro-angiogenic gene expression at times pi. (**e**) Protein levels of interleukin-6 (IL-6), (**f**) angiopoietin-2 (Ang-2), (**g**) fibroblast growth factor-2 (FGF-2), (**h**) hepatocyte growth factor (HGF), (**i**) VEGF-A, and (**j**) matrix metalloproteinase-9 (MMP-9) in time-course experiments. Data represent summary of mean ± s.e.m. of two–three independent experiments with $n = 5$–9 mice per time point. $^{*}P < 0.1$, $^{**}P < 0.01$, $^{***}P < 0.001$, $^{****}P < 0.0001$ comparing infected mice to uninfected (UI) control animals as determined by one-way ANOVA followed by Dunnett's multiple comparisons test.

produced by corneal epithelial cells during HSV-1 infection,[25] contributes to HSV-1-induced lymphangiogenesis in the absence of TNF-α,[19] and was suppressed following DEX treatment (**Figure 5d**), we hypothesized IL-6 is active driving the progression of corneal vessel growth into the central cornea or maintenance thereof following viral resolution. To investigate this idea, HSV-1-infected mice received anti-IL-6 antibody or isotypic control (1 μg) in the conjunctiva at days 8, 10, and 12 pi. Upon evaluation of corneas at day 14 pi, there was a significant suppression of hemangiogenesis but not lymphangiogenesis (**Figure 7a–c**). Analysis of pro-angiogenic factor levels at day 14 pi revealed a selective loss of IL-6 expression without any appreciable effect on levels of other factors measured (**Figure 7d**). Extension of the time point to day 21 pi in animals treated with anti-IL-6 or isotypic control antibody demonstrated a block in the progression of blood and lymphatic vessel growth into the central cornea but did not resolve the neovascularization (**Figure 7e,g**). Protein array analysis of corneas at day 21 pi revealed no appreciable impact on any of the factors measured in the cornea comparing isotypic control to anti-IL-6 treatment groups (**Figure 7h**). Overall, temporal neutralization of IL-6 following viral clearance blocks progression of lymphatic and blood vessels in the cornea but does not contribute to the maintenance of established vessels. It is likely that other factors or a "master regulator" are (is) responsible for continuity of newly acquired corneal blood and lymphatic vessels following HSV-1 infection.

FGF-2 neutralization suppresses HSV-1-induced corneal neovascularization

FGF-2 has previously been shown to drive lymphangiogenesis in the cornea following exogenous addition.[26] Based on the findings described above in that DEX was found to suppress FGF-2 expression, which correlated with resolution of angiogenesis and lymphangiogenesis by day 21 pi, the role of FGF-2 in HSV-1-induced neovascularization was investigated. Following the same protocol as that using the neutralizing antibody to IL-6, anti-FGF-2 antibody-treated

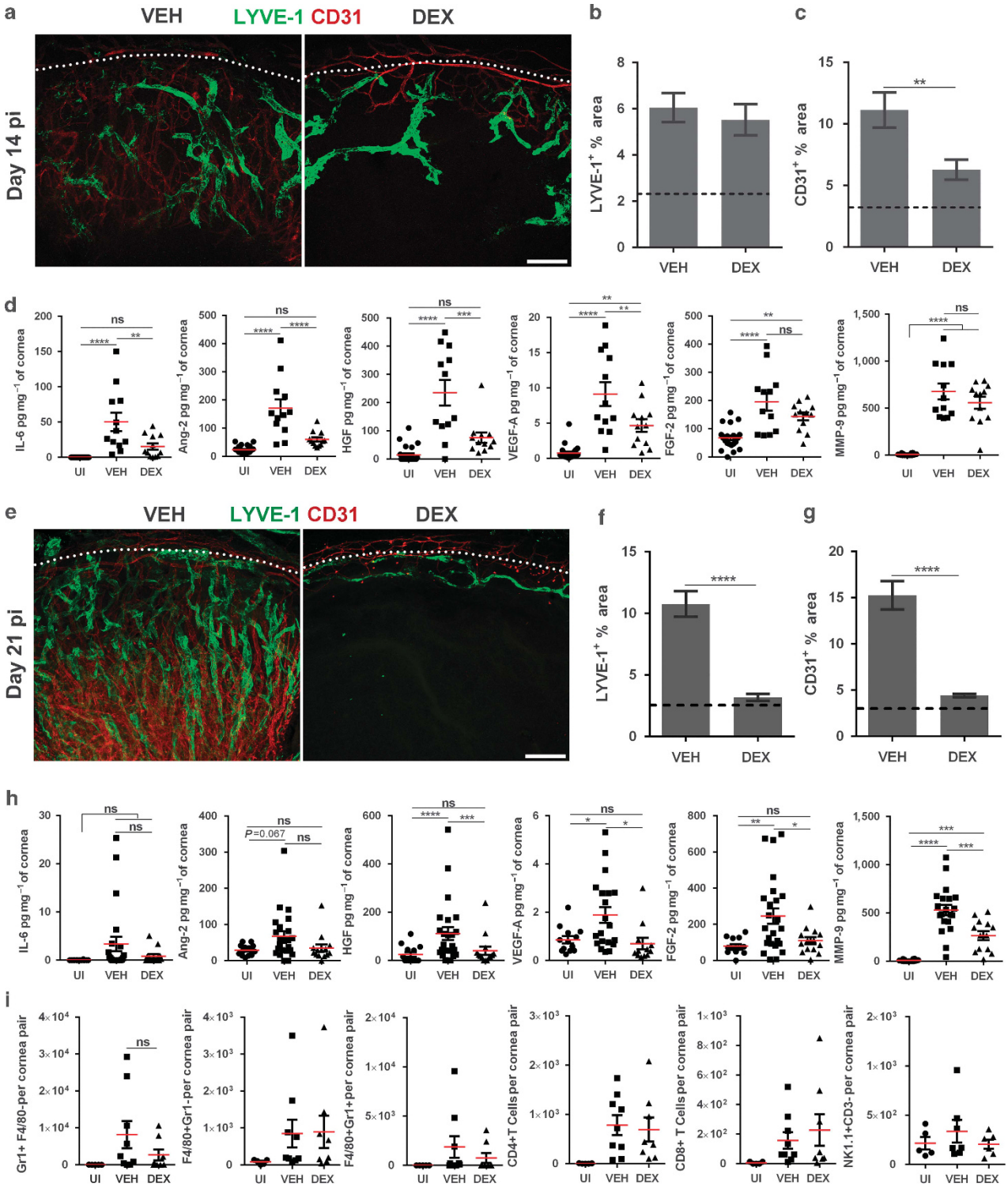

Figure 5 Dexamethasone suppresses HSV-1-induced corneal neovascularization in a time-dependent manner. A single bolus of vehicle or dexamethasone (DEX, 10 mg kg^{-1}) was given by intraperitoneal injection (ip) at day 10 pi. (**a**) Representative Z-stacked corneal images depicting lymphatic (green) and blood (red) vessels at day 14 pi comparing vehicle (VEH) to DEX-treated mice. Metamorph quantification of corneal area covered by (**b**) LYVE-1$^+$ lymphatic vessels, and (**c**) CD31$^+$ blood vessels per $\times$ 100 field of view. Bar = 200 μm. (**d**) Protein expression of pro-angiogenic factors at day 14 pi comparing VEH- to DEX-treated mice. (**e**) Representative Z-stacked corneal images depicting lymphatic (green) and blood (red) vessels at day 21 pi comparing VEH- to DEX-treated mice. Metamorph quantification of corneal area covered by (**f**) LYVE-1$^+$ lymphatic vessels, and (**g**) CD31$^+$ blood vessels per $\times$ 100 field of view. Bar = 200 μm. (**h**) Protein expression of pro-angiogenic factors at day 21 pi comparing VEH- to DEX-treated mice. (**i**) Leukocyte content in the cornea at day 21 pi indicating (from left to right) neutrophils, macrophages, inflammatory monocytes, CD4$^+$ T cells, CD8$^+$ T cells, and NK cells. Data represent the summary of mean ± s.e.m. of two independent experiments (**a**–**c** and **e**–**g**) with $n = 10$ corneas, three independent experiments (**d**,**h**) with $n = 6$–12 mice, two independent experiments (**i**) and $n = 5$–9 mice (**h**). $^{**}P < 0.01$, $^{****}P < 0.0001$ (**a**–**c**,**e**–**g**) as determined by Student's *t*-test. $^{*}P < 0.1$, $^{**}P < 0.01$, $^{***}P < 0.001$, $^{****}P < 0.0001$ (**d**,**h**) as determined by one-way ANOVA followed by Tukey's multiple comparisons test.

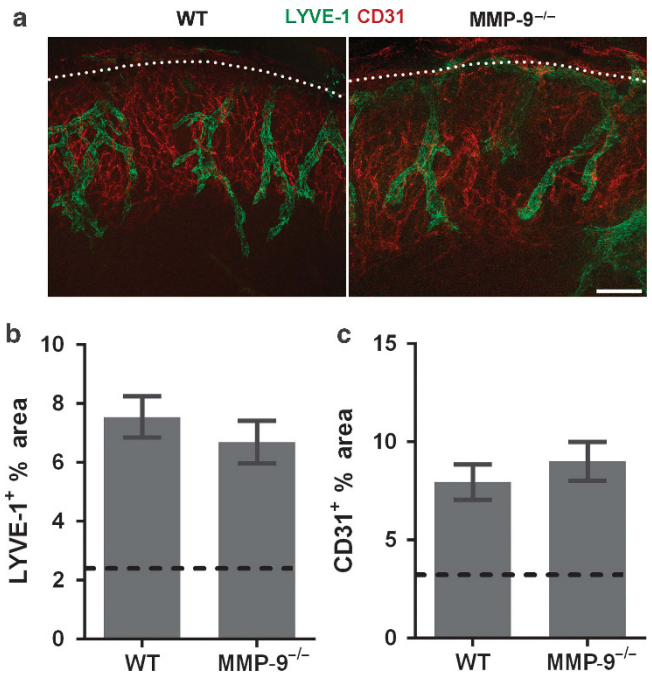

Figure 6 Matrix metalloproteinase-9 (MMP-9) is dispensable for HSV-1-induced corneal neovascularization. Wild-type (WT) C57BL/6 and MMP-9-deficient (MMP-9$^{-/-}$) mice were infected with HSV-1 and killed at day 14 pi to excise corneas for whole mount immunostaining of LYVE-1 and CD31. (**a**) Representative images of Z-stacked corneal whole mount indicating lymphatic (green) and blood (red) vessels. White dotted lines demarcate the corneolimbal region. Bar = 200 μm. Morphometric quantification of (**b**) LYVE-1 + lymphatic vessels, and (**c**) CD31 + blood vessels comparing WT to MMP$^{-/-}$ corneas. Data represents the summary of the mean ± s.e.m. of two independent experiments with eight corneas per group. Data were analyzed for significance ($P<0.05$) by Student's *t*-test.

mice displayed a significant reduction in lymph- and hem-angiogenesis when assessed at day 14 in comparison to isotype control antibody-treated animals (**Figure 8a–c**). Multiplex suspension array analysis revealed a significant reduction in the expression of all pro-angiogenic factors measured including IL-6, Ang-2, FGF-2, HGF, VEGF-A, and MMP-9 (**Figure 8d**). Suppression of corneal neovascularization following anti-FGF-2 antibody treatment was sustained at day 21 pi (**Figure 8e–g**). Concurrently, the levels of IL-6, HGF, VEGF-A, and FGF-2 were suppressed in this group as well, whereas the expression of Ang-2 and MMP-9 were unchanged in comparison to isotype-matched antibody-treated mice (**Figure 8h**). Notably, the elevated expression of MMP-9 in anti-FGF-2 antibody-treated corneas at this time point further underscores the finding that MMP-9 is dispensable for HSV-1-induced corneal neovascularization (**Figure 6**). Moreover, gelatin zymography assays[27] revealed that the active form of MMP-9 is found within the corneas of mice treated with anti-FGF-2 antibody at a level comparable to that found in mice treated with isotype-matched control antibody at day 21 pi (data not shown). Furthermore, anti-FGF-2 antibody treatment did not appear to have any appreciable impact on the influx of leukocytes into the cornea as compared to mice that received the isotype-matched antibody (**Figure 8i**). We interpret these results to suggest that the expression of the pro-angiogenic factors responsible for the progressive development and maintenance of corneal neovascularization following HSV-1 clearance is downstream of the FGF-2 receptor signaling cascade and that infiltrating leukocytes have a minimal direct role to play in this process.

Mast cells reside in the limbus of the cornea,[28] respond to HSV-1 infection,[28] and are a source of FGF-2.[29] To interrogate the role of mast cells in corneal nevascularization following HSV-1 infection, we performed immunohistochemistry of corneal whole mounts to probe for mast cells and FGF-2 expression at day 14 pi. We found that the mast cells were predominantly localized in the peripheral/limbal area of the cornea and co-localized with FGF-2 expression (**Supplementary Figure 1 online**). Yet, the vast majority of FGF-2 expression resided with other cells. Specifically, the FGF-2 staining was detected throughout the center cornea where mast cells were not visible.

FGF-2 neutralization fails to restore corneal sensitivity but partially improves visual acuity

The cornea is the most highly innervated tissue with sensory fibers that penetrate the corneal epithelium from a sub-basal nerve plexus.[30] Maintenance of this network is imperative for corneal integrity and optimal function.[31] Likewise, visual acuity is significantly impacted by inflammation including neovascularization of the cornea that occurs following HSV-1 infection.[32] Since there was a remarkable suppression of HSV-1-induced corneal neovascularization in mice treated with anti-FGF-2 antibody, functional aspect of visions were evaluated in these mice including corneal sensitivity and visual acuity. Time-course experiments revealed partial recovery of visual acuity in mice treated with FGF-2 antibody in comparison to the isotypic control antibody-treated group 14–21 days pi (**Figure 9a**). However, there was no substantial improvement in corneal sensation as measured by the blink reflex in mice that received anti-FGF-2 antibody treatment compared to those that received isotype-matched control antibody treatment (**Figure 9b**).

DISCUSSION

Developmental angiogenesis is a tightly regulated process that primarily depends on the concentration gradient of chemotactic and pro-angiogenic factors.[21,33] By comparison, inflammatory neovascularization is an unregulated phenomenon associated with the influx of activated leukocytes that extravasate/transmigrate from within the blood vessels to the tissue parenchyma. Tissue-infiltrating and resident leukocytes along with non-hematopoietic resident cells, including fibroblasts and mesenchymal cells, can all play intricate roles in angiogenesis.[9,34] In HSV-1-induced corneal neovascularization, a significant infiltration of leukocytes was observed after virus clearance from the cornea. The location of the infiltrating leukocytes past virus resolution revealed a predominant extravascular/posterior stroma confinement proximal to newly acquired blood and lymphatic vessels. However, the leukocytes

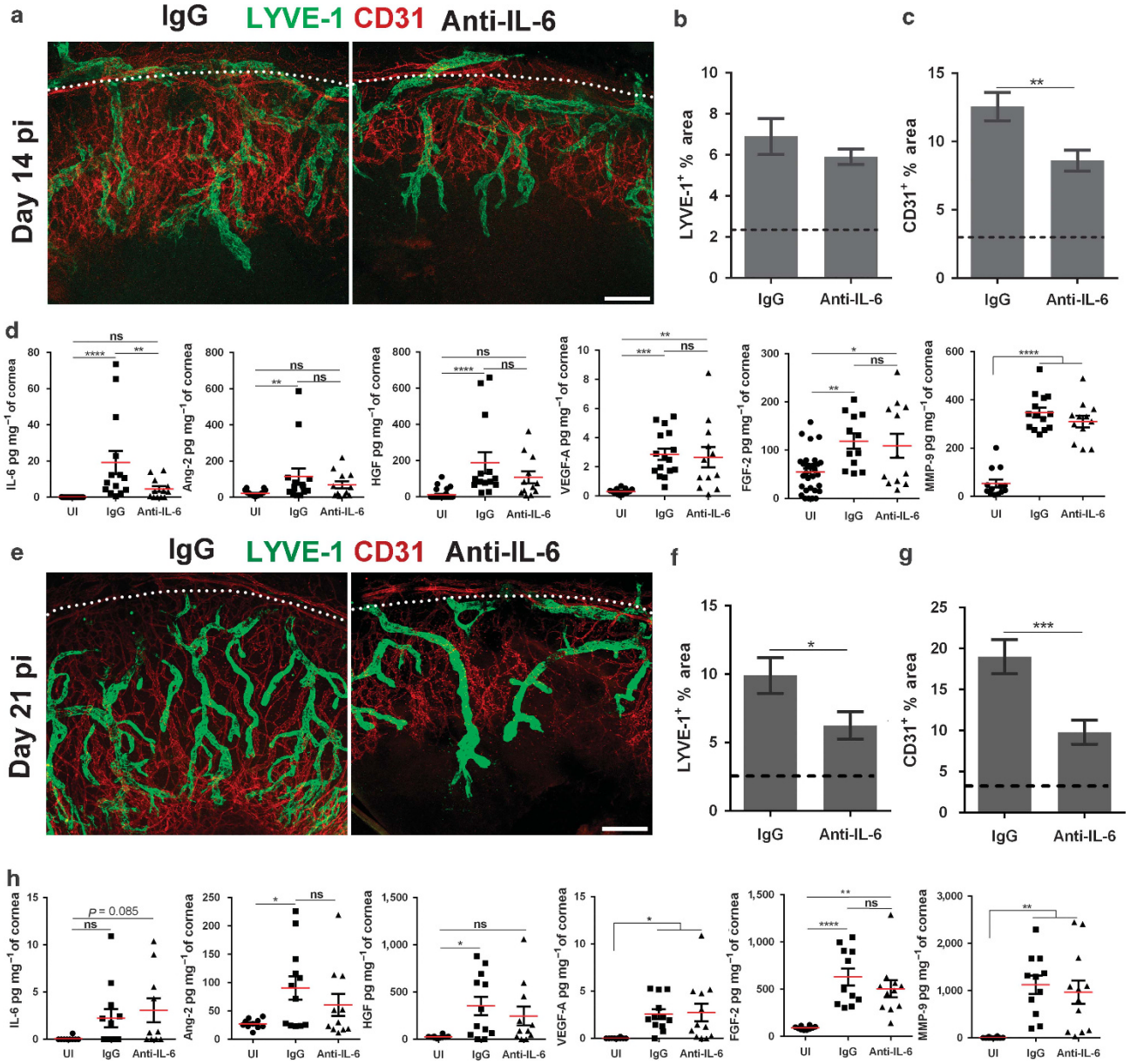

Figure 7 IL-6 neutralization blocks progression but does not induce regression of newly acquired lymphatic and blood vessels. Mice were infected and neutralizing antibody against IL-6 or isotype control antibody (1 μg/10 μl PBS) were injected subjconjunctivally at days 8, 10, and 12 pi. (**a**) Representative Z-stacked corneal images depicting lymphatic (green) and blood (red) vessels at day 14 pi comparing isotype control antibody (IgG) to anti-IL-6 antibody-treated mice. Metamorph quantification of corneal area containing (**b**) LYVE-1 $^{+}$ lymphatic vessels, and (**c**) CD31 $^{+}$ blood vessels per 100X field of view. (**d**) Protein expression of pro-angiogenic factors at day 14 pi comparing isotypic control to anti-IL-6 antibody-treated mice. (**e**) Representative Z-stacked corneal images depicting lymphatic (green) and blood (red) vessels at day 21 pi comparing IgG to anti-IL-6-treated mice. Metamorph quantification of corneal area covered by (**f**) LYVE-1 + lymphatic vessels and (**g**) CD31 $^{+}$ blood vessels per × 100 field of view. (**h**) Protein expression of pro-angiogenic factors at day 21 pi comparing isotypic control to anti-IL-6 antibody-treated mice. Data represent summary of the mean ± s.e.m. of two independent experiments (**a**–**c**,**e**–**g**) with $n = 10$ corneas, three independent experiments (**d**,**h**) with $n = 6$–12 mice. *$P < 0.1$, **$P < 0.01$, ***$P < 0.001$ (**a**–**c**,**e**–**g**) as determined by Student's *t*-test. *$P < 0.1$, **$P < 0.01$, ***$P < 0.001$, ****$P < 0.0001$ (**d**,**h**) as determined by one-way ANOVA followed by Tukey's multiple comparisons test. Bars = 200 μm.

did not appear to play a significant role in continued vascular genesis in the cornea. Specifically, depletion studies revealed the progressive development of blood and lymphatic vessels despite a significant loss of infiltrating immune cells including neutrophils, inflammatory monocytes, and a subpopulation of T cells. In contrast, pro-angiogenic factors, likely produced by resident cells under inflammatory conditions, were found to be significantly elevated following virus clearance. DEX intervention at the time of viral clearance resolved corneal lymph- and hemangiogenesis in a time-dependent fashion, and reduced the expression of several pro-angiogenic factors. Critical to the expression of these soluble factors and neovascularization was FGF-2 in which neutralization blocked progressive corneal vascularization and reduced expression of

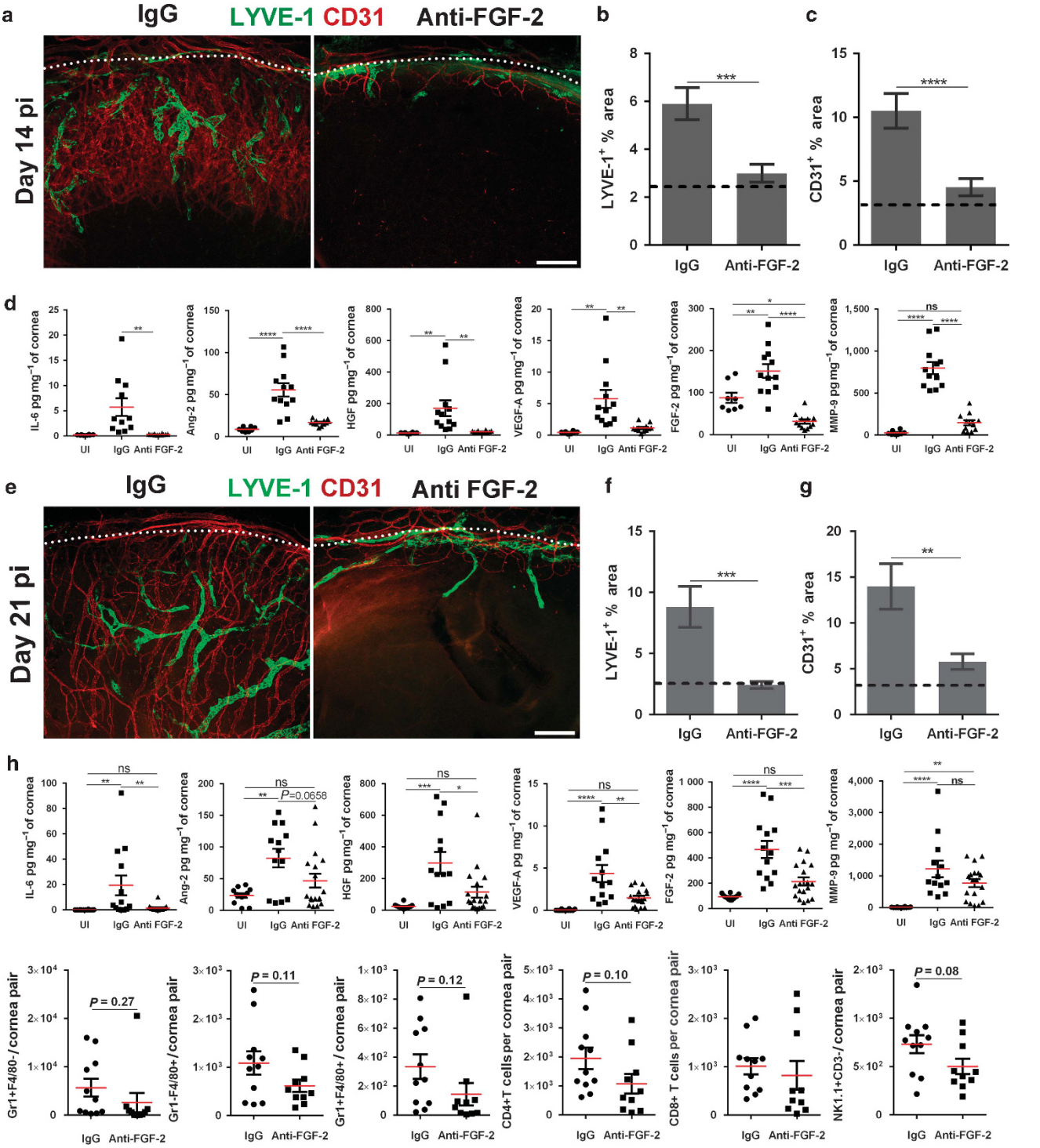

Figure 8 FGF-2 neutralization suppressed HSV-1-induced corneal neovascularization. Mice were inoculated with HSV-1, and neutralizing antibody against FGF-2 or isotype control antibody (5 μg per 10 μl PBS) were injected subjconjunctivally at days 8, 10, and 12 post infection (pi). (**a**) Representative Z-stacked corneal images depicting lymphatic (green) and blood (red) vessels at day 14 pi comparing isotype control antibody (IgG) to anti-FGF-2 antibody-treated mice. Metamorph quantification of corneal area containing (**b**) LYVE-1$^+$ lymphatic vessels, and (**c**) CD31$^+$ blood vessels per × 100 field of view. (**d**) Protein expression of pro-angiogenic factors at day 14 pi comparing isotypic control to anti-FGF-2 antibody-treated mice. (**e**) Representative Z-stacked corneal images depicting lymphatic (green) and blood (red) vessels at day 21 pi comparing isotypic control to anti-FGF-2 antibody-treated mice. Metamorph quantification of corneal area containing (**f**) LYVE-1$^+$ lymphatic vessels, and (**g**) CD31$^+$ blood vessels per × 100 field of view. (**h**) Protein expression of pro-angiogenic factors at day 21 pi comparing isotypic control to anti-FGF-2 antibody-treated mice. (**i**) Leukocyte content in the cornea at day 21 pi indicating (from left to right) neutrophils, macrophages, inflammatory monocytes, CD4$^+$ T cells, CD8$^+$ T cells, and NK cells. Data represent summary of mean ± s.e.m. of two independent experiments (**a**–**c**,**e**–**g**) with $n = 10$ corneas, three independent experiments (**d**,**h**) with $n = 6$–12 mice, three independent experiments (**h**,**i**) with $n = 10$–11 mice. $^{**}P < 0.01$, $^{**}P < 0.001$, $^{****}P < 0.0001$ (**a**–**c**,**e**–**g**,**i**) as determined by Student's *t*-test. $^{*}P < 0.1$, $^{**}P < 0.01$, $^{***}P < 0.001$, $^{****}P < 0.0001$ (**d**,**h**) as determined by one-way ANOVA followed by Tukey's multiple comparisons test. Bars = 200 μm.

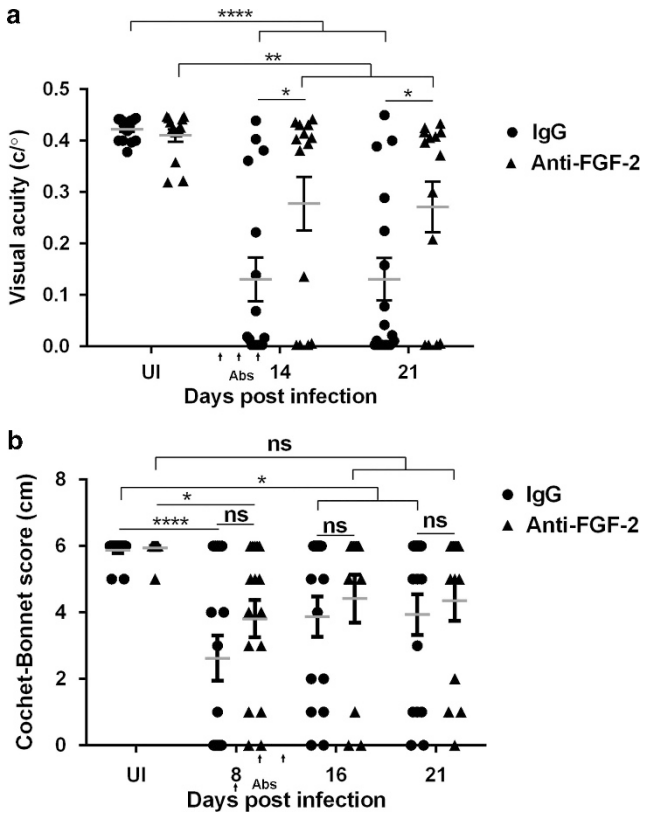

Figure 9 FGF-2 neutralization partially prevents the loss of visual acuity but not corneal sensation in HSV-1-infected mice. Mice were inoculated with HSV-1 or left uninfected. At days 8, 10, and 12 post infection (pi), anti-FGF-2 antibody or isotype-matched control antibody (5 μg per 10 μl PBS) were administered to infected mice by subconjunctival injection. (**a**) Functional vision of the mice was measured using opto-kinetic response tracking in optomotry at the indicated days pi. (**b**) Corneal sensation of mice was measured using a Cochet–Bonnet ethesiometer at the indicated days pi. Data represent the summary of mean ± s.e.m. of two independent experiments, $n = 7$–8 mice per group. $^{*}P < 0.1$, $^{**}P < 0.01$, $^{****}P < 0.0001$ as determined by two-way ANOVA followed by Dunnet's multiple comparisons test (comparing IgG and Anti-FGF-2-treated animals to uninfected control group).

several of the angiogenic factors including HGF, IL-6, and VEGF-A. These findings are summarized in **Figure 10**.

The lack of neutrophil involvement in HSV-1-induced corneal hemangiogenesis is in stark contrast to a previous study that reported a significant reduction in blood vessel genesis following the use of anti-Gr1 antibody to deplete neutrophils.[13] While we cannot readily rectify the differences between the two studies, the previous study employed a slit-lamp biomicroscope to score angiogenesis, which does not capitalize on the more precise and quantifiable method of assessing vessel growth in a normally avascular tissue such as the cornea by confocal microscopy as conducted in the present study. In the present study, anti-Gr1 antibody treatment did not deplete monocytes/macrophages or NK cells in the cornea such that these cells could contribute to corneal neovascularization. However, in terms of lymphangiogenesis, hematopoietic-derived cells have not been found to contribute to HSV-1-induced corneal lymphangiogenesis during acute infection.[8] In addition, DEX treatment or utilization of neutralizing antibody against FGF-2 blocked progressive corneal neovascularization without impacting leukocyte infiltration, including monocytes/macrophages and NK cells, to further underscore the lack of direct leukocyte contribution to HSV-1-induced corneal neovascularization.

Retention of newly formed vessels in tissue requires continued availability of pro-angiogenic factors.[33] Although it is not clear why several pro-angiogenic factors are expressed within the cornea after viral clearance, persistence of small amounts of HSV-1 antigen/DNA within the corneal resident cells may activate innate sensors that drive pro-inflammatory cytokine expression.[35,36] Mechanosensory stimuli may also elicit activation of innate immune signaling cascades as emilin-1, an anchoring filaments expressed on endothelial cells, anchors newly formed vessels within tissue parenchyma.[37]

MAP kinase and NF-κB pathways are the predominant source of pro-angiogenic factors, and DEX potently inhibits these signaling cascades.[38] The time-dependent suppression and regression of blood and lymphatic vessels by DEX intervention correlates with differential effects on the expression of pro-angiogenic factors. For example, FGF-2 and MMP-9 levels were not impacted by DEX at day 14 pi but DEX treatment did block IL-6, Ang-2, HGF, and VEGF-A. This selective effect on angiogenic factors at this time point coincided with a loss in hemangiogenesis but no apparent effect on lymphangiogenesis consistent with the idea that lymphangiogenesis can occur in the absence of hemangiogenesis.[26,39] By comparison, at day 21 pi, the lymphatic vessels regressed to baseline levels following DEX treatment with a significant inhibition of FGF-2 and MMP-9 protein expression. MMP-9 is a protease that degrades the extracellular matrix, promotes angiogenesis, and has previously been reported to facilitate HSV-1-induced corneal hemangiogenesis.[14] However, in the present study, no appreciable differences were observed in lymph- or hemangiogenesis comparing WT to MMP-9-deficient mice. Besides the differences in the use of different strains of mice, virus, and the inoculum, we attribute such contrary results to the variation in the technique used to quantify the neovessels in the entire cornea. Lee *et al.* used a biomicroscopic method to score hemangiogenesis, which may be subjective and may not be as accurate as laser-scanning confocal microscope analysis of Z-stacked corneal whole mounts used in this study.

IL-6 induces VEGF-A expression via the JAK/STAT pathway.[24] However, VEGF-A repression was not observed following IL-6 neutralization suggesting a compensatory mechanism of VEGF-A production. Neutralization of IL-6 did not impact any other pro-angiogenic factors measured despite exerting suppressive effects on growth progression of newly acquired corneal vessels. Such observation indicates direct effect of IL-6 on endothelial cells, which is consistent with other studies.[40,41]

FGF-2 is a potent heparin-binding growth factor that not only induces angiogenesis, but also stimulates mitogenic, proliferative, and migratory effects on various cell types.[42] It controls the expression of many different cytokines including IL-6,[43] VEGF-A,[42] HGF,[44] MMP-9,[45] and angiopoietin-2.[46]

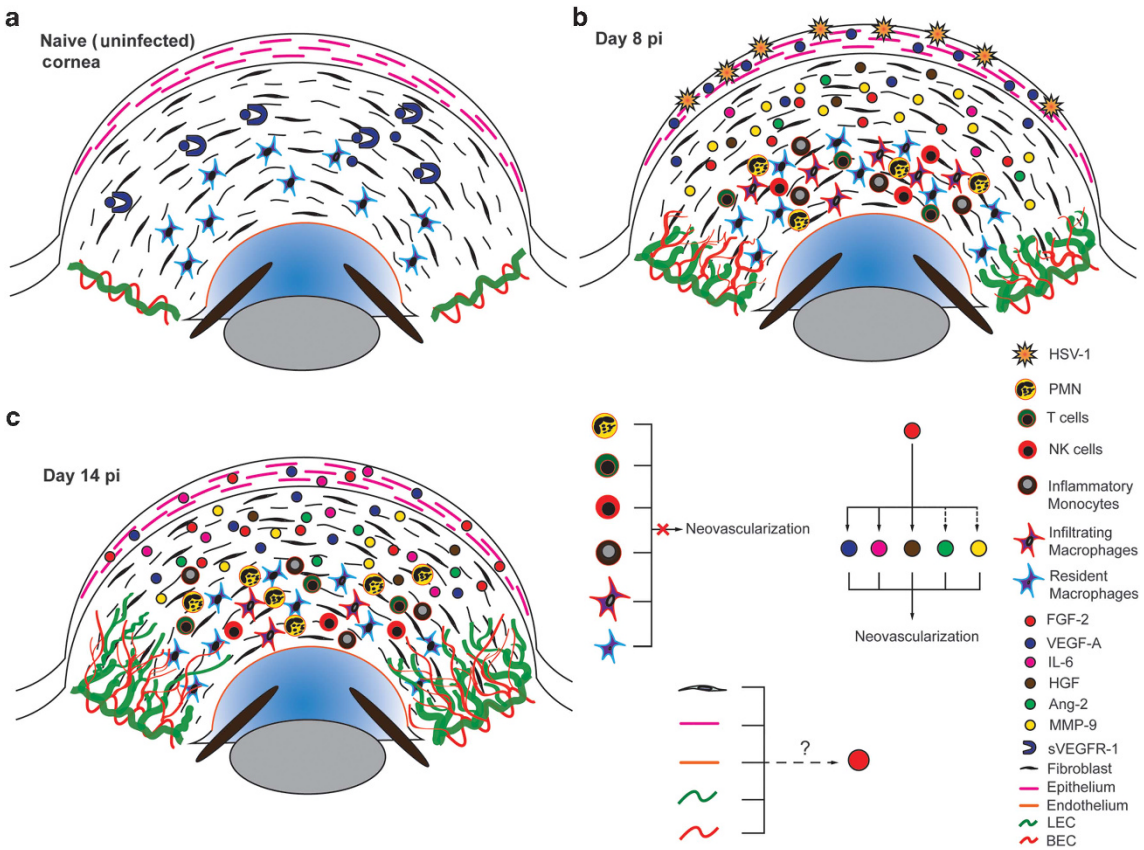

Figure 10 Schematic of HSV-1-induced corneal neovascularization. (**a**) Naive (uninfected) cornea exhibits basal level of VEGF-A, which is normally neutralized by soluble form of VEGFR-1 present within the cornea. Resident APCs (such as macrophages) decorate the posterior half of the corneal stroma. Limbal vasculature including blood and lymphatic vessels do not penetrate the center cornea under normal conditions. (**b**) Following HSV-1 infection, VEGF-A is predominantly produced by the infected corneal epithelial cells that drive corneal neovascularization. When the virus is still present in the corneal epithelium, immune cells including PMN, inflammatory monocytes, macrophages, T cells, and NK cells infiltrate the cornea. Various cytokines and growth factors such as IL-6, MMP-9, FGF-2, Ang-2, and HGF are also produced within the cornea leading to further inflammation. (**c**) When the virus is cleared in the cornea, the immune cells continue to infiltrate, pro-angiogenic factors continue to be produced, and neovascularization prolongs/sustains. However, immune cells do not have a major contribution to corneal neovascularization. MMP-9 is dispensable, IL-6 is necessary but not sufficient, whereas FGF-2 is crucial for HSV-1-induced corneal neovascularization. Importantly, FGF-2 controls the expression of VEGF-A, IL-6, Ang-2, HGF, and MMP-9. The primary source of FGF-2 may not be leukocytes. Instead, resident non-hematopoietic cells of the cornea including fibroblast (keratocytes), epithelium, endothelium, blood endothelial cells (BEC), and lymphatic endothelial cells (LEC) might play important roles in such processes.

Thus, FGF-2 may serve as a master regulator for other pro-angiogenic and -lymphangiogenic factors expressed during HSV-1 infection consistent with the results observed in the present study. Although leukocytes produce FGF-2 during inflammation,[29,47] they are most likely not the primary source of FGF-2, as depletion of the infiltrating leukocytes did not affect corneal neovascularization in this study. Such observation would indicate that the major sources of FGF-2 within the cornea after virus clearance are either the resident cells including fibroblasts, epithelium, keratocytes, and endothelium or the newly formed blood or lymphatic endothelial cells that encroach on the central cornea.

The impact of FGF-2 neutralization on HSV-1-induced corneal neovascularization was profound and correlated with improved visual outcome. Yet, corneal sensation was not rescued with the treatment. As FGF-2 is a potent factor involved in neurogenesis,[48] it is conceivable the downregulation of this factor negatively influences functional nerve regeneration. Consequently, even though FGF-2 neutralization as an adjunct therapy for HSV-1-induced neovascularization may be appealing, concomitant means to prevent nerve degeneration are critical. Collectively, the overall outcome of the present study highlights the central role for FGF-2 in the progression and maintenance of newly acquired blood and lymphatic vessels in the cornea of HSV-1-infected mice in the absence of infectious virions.

METHODS

Mice and infection. Six to eight-week-old male and female C57BL6/J and MMP-9 knockout mice were purchased from the Jackson Laboratory (Bar Harbor, ME). The mice were anesthetized with xylazine (6.6 mg kg^{-1}) and ketamine (100 mg kg^{-1}) prior to infection. Both corneas in each mouse were briefly killedwith a 27-gauge needle, tear film blotted, and 500 plaque forming units of HSV-1 (strain McKrae) in 3 µl of sterile phosphate buffered saline was inoculated on to the cornea. Animal protocols were approved by the University of Oklahoma Health Sciences Center's institutional animal care and use committee. All animals were handled with care according to the guidelines of American Association for Laboratory Animal Science.

Immunohistochemistry and confocal microscopy. Corneas were excised after cardiac perfusion with cold PBS of deeply anesthetized mice. The corneas were fixed in 4% paraformaldehyde for 30 min at 4° C followed by three 15 min washes with 1% PBS in 1% Triton X-100 (Sigma, St Louis, MO) at room temperature. The corneas were blocked with 10% normal donkey serum overnight at 4 °C. For primary staining, the corneas were incubated overnight with a cocktail of rabbit anti-mouse LYVE-1 (Abcam, Cambridge, MA), armenian hamster anti-mouse CD31 (Millipore, Billerica, MA), and rat anti-mouse CD45 (BD Pharmingen, San Jose, CA) in 0.1% PBS in 0.1% Trition X-100. For secondary staining, the corneas were incubated overnight with a cocktail of donkey anti-rabbit 488, goat anti-hamster TRITC, and goat anti-rat alexa flour 647 (all from Jackson Immunoresearch, West Grove, PA) in 0.1% PBS in 0.1% Trition X-100. The corneas were washed 5 ×, 30 min per wash in 0.1% PBS in 0.1% Trition X-100 at room temperature, and mounted on a glass slide after making radial cuts. For mast cell and FGF-2 co-staining, rabbit anti-mouse FGF-2 (Abcam) was used as primary antibody followed by an overnight incubation in a cocktail of donkey anti-rabbit TRITC (Jackson Immunoresearch) and FITC-conjugated Avidin (Biolegend, San Diego, CA). The corneas were then imaged with a laser-scanning confocal microscope, IX-81, FV500 (Olympus, Center Valley, PA).

Flow cytometry. Mice were killed at indicated times pi and tissues were collected. Corneas were digested in RPMI 1640 containing 10% fetal bovine serum, 1% antibiotic/antimicotic, and gentamicin at 37 °C as previously described.[28] Mandibular lymph node were dissociated with a 3 ml syringe-plunger head in the presence of media. Cell suspensions were passed through a 40-μ filter before staining. Single-cell suspensions were labeled with the following fluorochrome-conjugated monoclonal antibodies: rat anti-mouse CD45 efluor 450, rat anti-mouse CD3e FITC, rat anti-mouse CD4 APC, rat anti-mouse CD8 PE, rat anti-mouse CD3e PE-Cy7, rat anti-mouse NK1.1 FITC, rat anti-mouse CD11b APC, rat anti-mouse Ly6G FITC, rat anti-mouse Ly6C FITC (all from eBioscience, San Diego, CA), and rat anti-mouse F4/80 APC (Abcam). Labeled cells were washed in 1% bovine serum albumin in PBS and analyzed using a MACS Quant flow cytometer (Miltenyibiotec, Bergish Gladbach, Germany).

Neutrophil depletion. Mice were administered intraperitoneal injections of 0.5 mg anti-Gr1 or IgG2b isotype control (both from Bio X Cell, Lebanon, NH) in 100 μl PBS at days 7, 9, 11, and 13 pi. At day 14 pi, whole blood was collected from the mice via facial vein using an 18-gauge needle, and the mice were anesthetized and perfused with PBS via cardiac puncture. The whole blood underwent red blood cell lysis before cell surface labeling for flow cytometry to confirm neutrophil depletion.

3D deconvolution. Z-stacked images of the whole mount corneas were acquired using a laser-scanning confocal microscope, IX-81, FV500 (Olympus) with a step size of 1 μm and numerical aperture of 1.25 at a magnification of ×400. The images were processed to create 3D deconvolution using IMARIS software (Bitplane).

Gene and protein analysis. For gene array, corneas were processed using a magnetic bead-based Quantigene 2.0 multiplex kit (Affymetrix, Santa Clara, CA). Briefly, samples were lysed to extract RNA and incubated with specific target probes overnight. Signals were amplified with a hybridization technique, and detected using a luminex instrument (BioRad, Hercules, CA) after adding streptavidin with phycoerythrin as a substrate. For protein array, tissues were homogenized with a Tissuemiser (Fisher Scientific, Waltham, MA) in Tissue Protein Extraction Reagent (T-PER, Fisher Scientific) in the presence of 1 × Calbiochem protease inhibitor cocktail set I (Millipore). Homogenates were centrifuged in a microcentrifuge at 10 000 × g for 90 s at 4 °C, and the supernatants were evaluated for analyte content by multiplex (Millipore) or ELISA (R&D Systems, Minneapolis, MN) assays.

DEX and antibody treatment. Mice were given a single bolus of DEX (Sigma) by intraperitoneal injection at the concentration of 10 mg kg^{-1} or equivalent amount of vehicle (10% DMSO in PBS) at day 10 pi. Neutralizing monoclonal antibodies including 1 μg of anti-IL-6 (Biolegend; clone MP5-20F3) or rat IgG1, κ isotype control (Biolegend; clone RTK2071) in 10 μl PBS, and 5 μg of anti-FGF-2 (Millipore; clone bFM-1) or mouse IgG1, κ isotype control (Biolegend; clone MOPC-21) in 10 μl PBS were administered to mice by subconjunctival injection at days 8, 10, and 12 pi.

Functional vision measurement. Visual acuity was assessed by measuring the opto-kinetic tracking response provided by optomotry (CerebralMechanics) as previously described.[49] Briefly, each animal was placed on an elevated platform in a chamber surrounded by computer monitors and a camera above the animal. Visual stimulus including sine wave grating at 100% contrast in 3D space that rotated 360° in both directions around the subject was generated by the computer. As the gratings moved in clockwise or counterclockwise direction, the spatial frequency of the gratings was increased using a simple staircase method until no apparent head-tracking movement was observed. The highest spatial frequency at which the reflexive movements were observed was recorded as the threshold, i.e., cycles per degree. In this study, the minimum grating frequency tracked by the mice was 0.003 cycles per degree (essentially blind) and the maximum value was always below 0.5 cycles per degree. The reflexive movements of the head and neck were recorded by a masked observer to decode the values. Corneal sensitivity was measured using a Cochet–Bonnet esthesiometer as previously described.[50] Briefly, the non-anesthetized mice were presented with a monofilament in the esthesiometer with lengths ranging from 6.0 to 0.5 cm in order to observe a blink response. The length of the filament at which the blink response was observed was recorded for each eye. No blink response at 0.5 cm length of the filament was recorded as 0.

Statistics. Data from the time-course experiments comparing the mean ± s.e.m. at each time point to the uninfected sample were analyzed by one-way ANOVA followed by Dunnett's multiple comparisons test. Data comparing three groups at a given time point were analyzed by one-way ANOVA followed by Tukey's multiple comparisons test and groups of two were analyzed by Student's *t*-test. Data containing repeated measures at each time point (esthisiometry and OKT) were analyzed by two-way ANOVA followed by Dunnett's multiple comparisons test against the uninfected groups. Finally, two groups at each time point in time-course experiments were analyzed by multiple *t*-tests and statistical significance was determined using Holm–Sidak method. All data were presented as mean ± s.e.m. and analyzed using Prism software (GraphPad 6.0) and ComplexHeatmap package (Bioconductor version 3.3) available for R programming tool.

SUPPLEMENTARY MATERIAL is linked to the online version of the paper at http://www.nature.com/mi

ACKNOWLEDGMENTS

This work was supported by the National Institute of Health Grant R01 EY021238, P30 EY021725, and an unrestricted grant from Research to Prevent Blindness. The funding for IMARIS software was provided by grant from the Presbyterian Health Foundation.

AUTHOR CONTRIBUTIONS

H.R.G. designed, performed, and analyzed all experiments and wrote the manuscript. M.M.C. assisted with OKT experiments. K.B. designed and assisted with the time-course experiments for Figures 1–3. A.J.C.E. assisted with esthesiometry experiments and critiqued the manuscript. D.J.J.C. designed, critiqued, and wrote the manuscript, and supervised the work.

DISCLOSURE

The authors declare no conflict of interest.

REFERENCES

1. Streilein, J.W. Ocular immune privilege: therapeutic opportunities from an experiment of nature. *Nat. Rev. Immunol.* **3**, 879–889 (2003).
2. Ambati, B.K. *et al.* Corneal avascularity is due to soluble VEGF receptor-1. *Nature* **443**, 993–997 (2006).
3. Chang, J.-H. *et al.* Corneal neovascularization: an anti-VEGF therapy review. *Surv. Ophthalmol.* **57**, 415–429 (2012).
4. Hamrah, P., Huq, S.O., Liu, Y., Zhang, Q. & Dana, M.R. Corneal immunity is mediated by heterogeneous population of antigen-presenting cells. *J. Leukoc. Biol.* **74**, 172–178 (2003).
5. Griffith, T.S., Brunner, T., Fletcher, S.M., Green, D.R. & Ferguson, T.A. Fas ligand-induced apoptosis as a mechanism of immune privilege. *Science* **270**, 1189–1192 (1995).
6. Kuffova, L. *et al.* High-risk corneal graft rejection in the setting of previous corneal herpes simplex virus (HSV)-1 infection. *Investig. Opthalmol. Vis. Sci.* **57**, 1578 (2016).
7. Farooq, A.V. & Shukla, D. Herpes simplex epithelial and stromal keratitis: an epidemiologic update. *Surv. Ophthalmol.* **57**, 448–462 (2012).
8. Wuest, T.R. & Carr, D.J.J. VEGF-A expression by HSV-1-infected cells drives corneal lymphangiogenesis. *J. Exp. Med.* **207**, 101–115 (2010).
9. Cursiefen, C. *et al.* VEGF-A stimulates lymphangiogenesis and hemangiogenesis in inflammatory neovascularization via macrophage recruitment. *J. Clin. Invest.* **113**, 1040–1050 (2004).
10. Maruyama, K. *et al.* Inflammation-induced lymphangiogenesis in the cornea arises from CD11b-positive macrophages. *J. Clin. Invest.* **115**, 2363–2372 (2005).
11. Wuest, T., Zheng, M., Efstathiou, S., Halford, W.P. & Carr, D.J.J. The herpes simplex virus-1 transactivator infected cell protein-4 drives VEGF-A dependent neovascularization. *PLoS Pathog.* **7**, e1002278 (2011).
12. Conrady, C.D., Zheng, M., Stone, D.U. & Carr, D.J.J. CD8+ T cells suppress viral replication in the cornea but contribute to VEGF-C induced lymphatic vessel genesis. *J. Immunol.* **189**, 425–432 (2012).
13. Suryawanshi, A. *et al.* Ocular neovascularization caused by HSV-1 infection results from breakdown of binding between VEGF-A and its soluble receptor. *J. Immunol.* **186**, 3653–3665 (2011).
14. Lee, S., Zheng, M., Kim, B. & Rouse, B.T. Role of matrix metalloproteinase-9 in angiogenesis caused by ocular infection with herpes simplex virus. *J. Clin. Invest.* **110**, 1105–1111 (2002).
15. Bergers, G. *et al.* Matrix metalloproteinase-9 triggers the angiogenic switch during carcinogenesis. *Nat. Cell Biol.* **2**, 737–744 (2000).
16. Divito, S.J. & Hendricks, R.L. Activated inflammatory infiltrate in HSV-1-infected corneas without herpes stromal keratitis. *Invest. Ophthalmol. Vis. Sci.* **49**, 1488–1495 (2008).
17. Thomas, J., Gangappa, S., Kanangat, S. & Rouse, B.T. On the essential involvement of neutrophils in the immunopathologic disease: herpetic stromal keratitis. *J. Immunol.* **158**, 1383–1391 (1997).
18. Bryant-Hudson, K.M. & Carr, D.J.J. CXCL1-deficient mice are highly sensitive to pseudomonas aeruginosa but not herpes simplex virus type 1 corneal infection. *Invest. Ophthalmol. Vis. Sci.* **53**, 6785–6792 (2012).
19. Bryant-Hudson, K.M., Gurung, H.R., Zheng, M. & Carr, D.J.J. Tumor necrosis factor alpha and interleukin-6 facilitate corneal lymphangiogenesis in response to herpes simplex virus 1 infection. *J. Virol.* **88**, 14451–14457 (2014).
20. Tonini, T., Rossi, F. & Claudio, P.P. Molecular basis of angiogenesis and cancer. *Oncogene* **22**, 6549–6556 (2003).
21. Tammela, T. & Alitalo, K. Lymphangiogenesis: molecular mechanisms and future promise. *Cell* **140**, 460–476 (2010).
22. Gross, J. *et al.* Inhibition of tumor growth, vascularization, and collagenolysis in the rabbit cornea by medroxyprogesterone. *Proc. Natl. Acad. Sci. USA* **78**, 1176–1180 (1981).
23. Nakao, S. *et al.* Dexamethasone inhibits interleukin-1β-induced corneal neovascularization. *Am. J. Pathol.* **171**, 1058–1065 (2007).
24. Cohen, T., Nahari, D., Cerem, L.W., Neufeld, G. & Levi, B.-Z. Interleukin 6 induces the expression of vascular endothelial growth factor. *J. Biol. Chem.* **271**, 736–741 (1996).
25. Li, H. *et al.* Herpes simplex virus 1 infection induces the expression of proinflammatory cytokines, interferons and TLR7 in human corneal epithelial cells. *Immunology* **117**, 167–176 (2006).
26. Chang, L.K. *et al.* Dose-dependent response of FGF-2 for lymphangiogenesis. *Proc. Natl. Acad. Sci. USA* **101**, 11658–11663 (2004).
27. Hu, X. & Beeton, C. Detection of functional matrix metalloproteinases by zymography. *J. Vis. Exp.*, pii: 2445; doi: 10.3791/2445 (2010).
28. Royer, D.J., Zheng, M., Conrady, C.D. & Carr, D.J.J. Granulocytes in ocular HSV-1 infection: opposing roles of mast cells and neutrophils. *Investig. Opthalmol. Vis. Sci.* **56**, 3763 (2015).
29. Qu, Z. *et al.* Mast cells are a major source of basic fibroblast growth factor in chronic inflammation and cutaneous hemangioma. *Am. J. Pathol.* **147**, 564–573 (1995).
30. Müller, L.J., Marfurt, C.F., Kruse, F. & Tervo, T.M.T. Corneal nerves: structure, contents and function. *Exp. Eye Res.* **76**, 521–542 (2003).
31. Beuerman, R.W. & Schimmelpfennig, B. Sensory denervation of the rabbit cornea affects epithelial properties. *Exp. Neurol.* **69**, 196–201 (1980).
32. Streilein, J.W., Dana, M.R. & Ksander, B.R. Immunity causing blindness: five different paths to herpes stromal keratitis. *Immunol. Today* **18**, 443–449 (1997).
33. Carmeliet, P. Mechanisms of angiogenesis and arteriogenesis. *Nat. Med.* **6**, 389–395 (2000).
34. Kreuger, J. & Phillipson, M. Targeting vascular and leukocyte communication in angiogenesis, inflammation and fibrosis. *Nat. Rev. Drug Discov.* **15**, 125–142 (2016).
35. Hemmi, H. *et al.* A Toll-like receptor recognizes bacterial DNA. *Nature* **408**, 740–745 (2000).
36. Pearlman, E. *et al.* Host defense at the ocular surface. *Int. Rev. Immunol.* **32**, 4–18 (2013).
37. Danussi, C. *et al.* Emilin1 deficiency causes structural and functional defects of lymphatic vasculature. *Mol. Cell. Biol.* **28**, 4026–4039 (2008).
38. Chi, G. *et al.* Suppression of MAPK and NF-κB pathways by limonene contributes to attenuation of lipopolysaccharide-induced inflammatory responses in acute lung injury. *Inflammation* **36**, 501–511 (2013).
39. Nakao, S. *et al.* Lymphangiogenesis and angiogenesis: concurrence and/or dependence? Studies in inbred mouse strains. *FASEB J.* **24**, 504–513 (2010).
40. Fan, Y. *et al.* Interleukin-6 stimulates circulating blood-derived endothelial progenitor cell angiogenesis *in vitro*. *J. Cereb. Blood Flow Metab.* **28**, 90–98 (2008).
41. Gopinathan, G. *et al.* Interleukin-6 stimulates defective angiogenesis. *Cancer Res.* **75**, 3098–3107 (2015).
42. Seghezzi, G. *et al.* Fibroblast growth factor-2 (FGF-2) induces vascular endothelial growth factor (VEGF) expression in the endothelial cells of forming capillaries: an autocrine mechanism contributing to angiogenesis. *J. Cell Biol.* **141**, 1659–1673 (1998).
43. Delrieu, I., Arnaud, E., Ferjoux, G., Bayard, F. & Faye, J.C. Overexpression of the FGF-2 24-kDa isoform up-regulates IL-6 transcription in NIH-3T3 cells. *FEBS Lett.* **436**, 17–22 (1998).
44. Blanquaert, F., Delany, A.M. & Canalis, E. Fibroblast growth factor-2 induces hepatocyte growth factor/scatter factor expression in osteoblasts. *Endocrinology* **140**, 1069–1074 (1999).
45. Liu, J.-F., Crépin, M., Liu, J.-M., Barritault, D. & Ledoux, D. FGF-2 and TPA induce matrix metalloproteinase-9 secretion in MCF-7 cells through PKC activation of the Ras/ERK pathway. *Biochem. Biophys. Res. Commun.* **293**, 1174–1182 (2002).
46. Fujii, T. & Kuwano, H. Regulation of the expression balance of angiopoietin-1 and angiopoietin-2 by Shh and FGF-2. *In Vitro Cell. Dev. Biol. Anim.* **46**, 487–491 (2010).
47. Henke, C. *et al.* Macrophage production of basic fibroblast growth factor in the fibroproliferative disorder of alveolar fibrosis after lung injury. *Am. J. Pathol.* **143**, 1189–1199 (1993).
48. Jin, K. *et al.* FGF-2 promotes neurogenesis and neuroprotection and prolongs survival in a transgenic mouse model of Huntington's disease. *Proc. Natl. Acad. Sci. USA* **102**, 18189–18194 (2005).
49. Redfern, W.S. *et al.* Evaluation of a convenient method of assessing rodent visual function in safety pharmacology studies: effects of sodium iodate on visual acuity and retinal morphology in albino and pigmented rats and mice. *J. Pharmacol. Toxicol. Methods* **63**, 102–114 (2011).
50. Chucair-Elliott, A.J., Zheng, M. & Carr, D.J.J. Degeneration and regeneration of corneal nerves in response to HSV-1 infection. *Invest. Ophthalmol. Vis. Sci.* **56**, 1097–1107 (2015).